

# Quantum-mechanical interference between optical transitions and the effect of laser phase noise

J. C. Camparo<sup>1</sup> and P. Lambropoulos<sup>2,3</sup>

<sup>1</sup>*Electronics Technology Center, The Aerospace Corporation, P.O. Box 92957, Los Angeles, California 90009*

<sup>2</sup>*Max-Planck-Institut für Quantenoptik, D-1046, Garching, Germany*

<sup>3</sup>*Foundation for Research and Technology, Hellas Institute, Institute of Electronic Structure & Laser, P.O. Box 1527, Heraklion 71110, Crete, Greece and Department of Physics, University of Crete, Crete, Greece*

(Received 2 August 1996)

We consider three-photon–one-photon phase control of resonance-enhanced photoionization with a phase-diffusion field. As is well known, control is achieved because excitation via the fundamental field interferes with excitation via the third harmonic field, and the form of the interference (i.e., constructive or destructive) depends on the relative phase difference between the two fields. In the problem, the stochastic nature of the field influences control because the propagation constant of a dispersive medium depends on the field's fluctuating frequency. Here, we approach the influence of laser phase noise on control via (i) a physically intuitive zeroth-order approximation, (ii) first-order perturbation theory, and (iii) numerical simulation. Our results show that first-order perturbation theory is not attractive for the study of this problem, since it requires the evaluation of very high order correlation functions associated with the fundamental field's fluctuating frequency. More importantly, however, numerical simulation demonstrates that highly efficient control can be attained even in the presence of very large linewidth fields. [S1050-2947(96)08712-4]

PACS number(s): 32.80.Rm, 32.80.Qk

## I. INTRODUCTION

Over the past several years, there has been a growing interest among physicists and chemists with interference effects arising from independent pathways of optical excitation. In part, this interest stems from a desire to direct the explicit course of atomic and molecular processes. Since independent pathways of optical excitation can interfere, and since the constructive or destructive nature of this interference can be controlled via the relative phase of the fields involved, it may be possible to use laser-phase as a tool for tailoring atomic and molecular wave functions and hence for manipulating branching ratios. One of the better known methods for achieving this phase control is known as the “3+1” technique [1,2], and it has motivated much theoretical and experimental effort.

In 3+1 phase control, an optical transition is excited via a three-photon and a one-photon pathway. The field at the fundamental frequency  $\omega_1$  has a phase  $\phi_1$ , while the third harmonic field with frequency  $\omega_3$  has a phase  $\phi_3$ . The rate of excitation is proportional to the square of the total transition amplitude, and hence is proportional to  $[1 + \cos(\phi_3 - 3\phi_1)]$ . (We have assumed equal one-photon and three-photon transition amplitudes, and we have ignored any constant phase difference between the two quantum-mechanical paths, since even in those cases where it might be nonzero it can be incorporated into the relative phase difference between the two fields.) Thus, control of the relative phase  $\theta \equiv \phi_3 - 3\phi_1$  yields control over the atomic or molecular wave function. To date, the 3+1 technique has been demonstrated via bound-bound transitions in both atomic [3] and molecular systems [4]; it has been extended to two-photon–four-photon interfering pathways [5]; it has been observed with bound-continuum transitions in polyatomic molecules [6], and it has been used as a means of measuring gas-phase refractive in-

stances [7]. Moreover, a density-matrix description of multiple interfering pathways has been developed [8], allowing the investigation of phase control with strong fields, and this has been successfully employed to investigate interfering pathways associated with discrete states imbedded in a continuum [9].

Even without detailed analysis, one might expect the coherence characteristics of the field employed in the 3+1 technique to significantly influence the degree of control. Consider the standard 3+1 phase-control experiment shown in Fig. 1. There, a field is tripled in some nonlinear medium before passing through a dispersive medium of length  $L$ . [We assume that  $\omega_3(t)$  equals  $3\omega_1(t)$  for all  $t$ , and take  $n_i$  as the refractive index of the dispersive medium at either the fundamental frequency  $n_1$ , or third harmonic frequency  $n_3$ .] If the fundamental is a phase-diffusion field (PDF), where

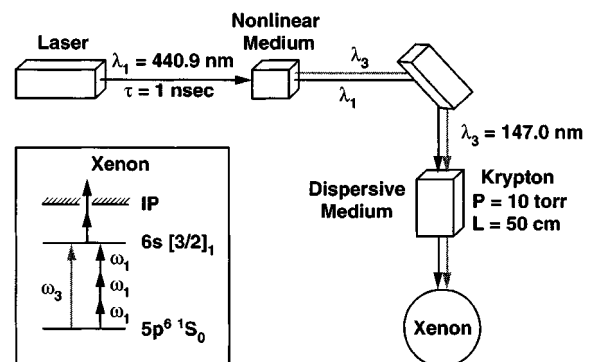


FIG. 1. Standard 3+1 phase-control experiment. A fundamental field from a laser is tripled in a nonlinear medium, and then both the fundamental and third harmonic pass through a dispersive medium. Since the refractive indices of the dispersive medium for the fundamental and third harmonic fields are different, a relative phase difference between the two fields is created. Our numerical simulations consider 3+1 phase-control of xenon photoionization.

the stochastic characteristics of the field derive solely from the stochastic characteristics of the field's phase,  $\psi$  [or equivalently from the field's instantaneous frequency,  $\omega(t) \equiv \dot{\psi}(t)$ ], then at the exit of the dispersive medium the  $i$ th field may be written as

$$\begin{aligned} E_i(t) &= \varepsilon_i \sin[\bar{\omega}_i t + \delta\psi_i(t) + \bar{\phi}_i + \delta\phi_i(t)] \\ &\cong \varepsilon_i \sin\{[\bar{\omega}_i + \delta\omega_i(t)]t + \bar{\phi}_i + \delta\phi_i(t)\}. \end{aligned} \quad (1)$$

Here,  $\bar{\omega}$  is the average field frequency,  $\delta\psi(t)$  is a mean-zero stochastic phase variation of the field,  $\delta\omega(t)$  is a mean-zero stochastic frequency fluctuation of the field, and  $\phi(t)$  is the added phase arising from passage through the dispersive medium. Due to the fact that the dispersive medium's propagation constant depends on frequency, this added phase is a stochastic quantity by virtue of the stochastic nature of the laser frequency. Consequently, the added phase is written as the sum of an average added phase,  $\bar{\phi}$ , and a mean-zero stochastic added-phase variation,  $\delta\phi(t)$ :  $\phi(t) = \bar{\phi} + \delta\phi(t)$ , where

$$\delta\phi_i(t) = \frac{n_i \delta\omega_i(t)L}{c}. \quad (2)$$

Thus, the relative phase difference between the two fields is a stochastic variable:  $\theta(t) = \theta_0 + \delta\theta(t)$ , where

$$\theta_0 = \frac{3\bar{\omega}_1 L}{c} [n_3 - n_1] \quad (3a)$$

and

$$\delta\theta(t) = \frac{3\delta\omega_1(t)L}{c} [n_3 - n_1]. \quad (3b)$$

In the following sections of this paper we will explore the influence of these stochastic variations on the phase control of photoionization, and show that significant control can be attained even in the presence of large linewidth PDF's. In Sec. II, we will outline the specific experiment to be simulated, and discuss a physically intuitive zeroth-order approximation for the effect of laser phase fluctuations on control. Then in Sec. III we will present a first-order perturbation theory treatment of the problem, and demonstrate that the zeroth-order approximation requires an unphysical decorrelation between  $\delta\omega$  and  $\delta\theta$ . Finally, in Sec. IV we will present results from numerical simulations of phase control with both a weak and strong PDF. In the case of a weak PDF, we will find that even though the zeroth-order approximation is not exact, it is a very reasonable approximation up to very large linewidth PDF's under the experimental conditions examined here. In the case of strong fields, we will show that the results are qualitatively similar to the weak field case, though the ac Stark shift of the levels plays a significant role.

## II. ZERO-ORDER APPROXIMATION

To connect our analysis to realizable systems, and for our latter numerical computations, we consider the specific case of xenon's  $|5p^6 \ ^1S_0\rangle \rightarrow |6s[3/2]_1\rangle$  transition excited via a one-photon and three-photon pathway as illustrated in Fig.

TABLE I. Parameters associated with the excitation of xenon's  $|5p^6 \ ^1S_0\rangle \rightarrow |6s[3/2]_1\rangle$  transition computed via MQDT. The intensity  $I$  is in units of  $\text{W}/\text{cm}^2$ .

Parameter	Value ( $\text{sec}^{-1}$ )
Three-photon Rabi frequency, $\Omega_1$	$5 \times 10^{-7} I^{3/2}$
$ 6s[3/2]_1\rangle$ two-photon ionization rate, $\gamma_{\text{ion}}$	$7 \times 10^{-13} I^2$
Transition ac stark shift coefficient, $\kappa^a$	$+36(I)$ or $0$
$ 6s[3/2]_1\rangle$ decay rate, $\gamma_2$	$5 \times 10^8$

<sup>a</sup>The ac Stark shift coefficient corresponds to the shift of the ground state, and was estimated from the ground state polarizability and not MQDT. MQDT does indicate, though, that the excited state ac Stark shift coefficient is small by comparison.

1:  $\lambda_1 = 440.9$  nm and  $\lambda_3 = 147.0$  nm. Due to the fact that the  $\lambda_1$  field will be much more intense than the  $\lambda_3$  field, so as to keep the two excitation amplitudes comparable, the  $6s[3/2]_1$  state is ionized predominantly via two photons from the  $\lambda_1$  field, and the total amount of photoionization is the signal of interest. Moreover, consistent with experiment [4], krypton is taken as the dispersive medium with a nominal pressure of 10 torr and a path length of 50 cm. Then, interpolating the data of Leonard [10] and Chashchina and Shreider [11], we have  $n_{\text{Kr}}(\lambda_1) - 1 = 4.4 \times 10^{-4}$  and  $n_{\text{Kr}}(\lambda_3) - 1 = 7.1 \times 10^{-4}$ . Thus,  $\delta\theta(t) = \alpha \delta\omega(t)$ , where  $\alpha$  equals  $1.8 \times 10^{-14}$  sec. Other parameters associated with this system, calculated using MQDT [12], are collected in Table I.

As discussed above, the total transition rate for excitation from the ground state to the  $|6s[3/2]_1\rangle$  state is found by adding and then squaring the separate transition amplitudes for the two optical excitation pathways. Assuming equal excitation amplitudes, and including any intrinsic phase delay between the two paths in  $\theta_0$ , a zeroth-order approximation for the total fluctuating excitation rate,  $\Gamma_0$ , can be written as

$$\Gamma_0(\theta_0, t) \sim 1 + \cos[\theta_0 + \delta\theta(t)] = 1 \pm \cos[\alpha \delta\omega_1(t)], \quad (4)$$

where the plus and minus signs refer to  $\theta_0 = 0$  and  $\pi$ , respectively. The average excitation rate is then obtained by averaging  $\Gamma$  over  $\delta\omega_1$ :

$$\langle \Gamma(\theta_0) \rangle_0 \sim 1 \pm \int_{-\infty}^{\infty} P(\delta\omega_1) \cos(\alpha \delta\omega_1) d[\delta\omega_1]. \quad (5)$$

In this equation  $P(\delta\omega_1)$  is the Gaussian probability distribution for the frequency fluctuations of the  $\lambda_1$  field, and for a PDF

$$P(\delta\omega_1) = \frac{1}{\sqrt{2\pi\gamma\beta}} \exp\left[-\frac{(\delta\omega_1)^2}{2\gamma\beta}\right], \quad (6a)$$

where  $\gamma$  and  $\beta$  are defined by the correlation function of the laser frequency fluctuations:

$$\langle \delta\omega_1(t) \delta\omega_1(t - \tau) \rangle = \gamma\beta e^{-\beta|\tau|}. \quad (6b)$$

Here,  $2\gamma$  essentially defines the linewidth of the field (FWHM), and  $\beta$  is a parameter describing the non-Lorentzian falloff of the field's line-shape wings [13]. (For future reference we note that if  $\beta$  is proportional to  $\gamma$ , then the spectral profile of the field maintains its shape as the

field's linewidth varies). Evaluating the integral of Eq. (5) yields the zeroth-order approximation:

$$\langle \Gamma(\theta_0) \rangle_0 \sim 1 \pm \exp\left[-\frac{\alpha^2 \gamma \beta}{2}\right]. \quad (7)$$

In the limit that  $\alpha^2 \gamma \beta \ll 1$ , which is the limit of physical interest,  $\langle \Gamma(0) \rangle_0$  is approximately constant, while  $\langle \Gamma(\pi) \rangle_0$  is a monotonically increasing function of  $\gamma \beta$  [i.e.,  $\langle \Gamma(\pi) \rangle_0 \sim \alpha^2 \gamma \beta / 2$ ].

We define the contrast of phase control as the ratio of constructive to destructive interference signals, and parametrize the contrast by its logarithm,  $\zeta$ . Thus, as our signal is the degree of photoionization, which is proportional to the excitation rate in weak fields,

$$\zeta_0 = \log_{10} \left[ \frac{\langle \Gamma(0) \rangle_0}{\langle \Gamma(\pi) \rangle_0} \right] \cong \log_{10} \left[ \frac{4}{\alpha^2 \gamma \beta} \right], \quad (8)$$

where we have assumed that  $\alpha^2 \gamma \beta \ll 1$ . Consistent with intuition, the zeroth-order approximation predicts that  $\zeta_0$  is a monotonically decreasing function of the field linewidth parameter,  $\gamma$ ; and that for  $\beta$  proportional to  $\gamma$ ,  $\zeta_0 \sim -\log_{10}[\gamma]$ .

### III. FIRST-ORDER PERTURBATION THEORY

An inherent assumption of the zeroth-order approximation is that the excitation rate at time  $t$  only depends on the relative phase difference between the two excitation pathways at that particular instant. This assumption, however, is questionable on physical grounds. Labeling the excited state as  $|2\rangle$  and the ground state as  $|1\rangle$ , the probability of a  $|1\rangle \rightarrow |2\rangle$  transition at time  $t$  will depend on the atomic state at that instant. This in turn depends on previous probabilities for  $|1\rangle \rightarrow |2\rangle$  transitions, since the atom does not have a  $\delta$ -function response to an impulsive perturbation. Thus, in general we expect  $\langle \Gamma(\theta_0, t) \rangle$  to depend on  $\theta(t' < t)$ . In this section, we employ first-order perturbation theory to investigate this issue by computing a first-order approximation to the contrast,  $\zeta_1$ .

Since the standard density-matrix equations describing an  $n$ -photon transition between two discrete states [14,15] can be used to define an effective  $n$ -photon perturbation,  $V^{(n)}$ , we write a total effective perturbation for phase control as the sum of a one-photon and three-photon perturbation:  $V^{(1,3)} = V^{(1)} + V^{(3)}$ . The diagonal components of  $V^{(n)}$  are related to the individual levels' ac Stark shifts, while the off-diagonal components are determined by the  $n$ -photon Rabi frequency coupling the two levels. In particular, for the present case

$$\begin{aligned} V_{21}^{(1,3)} &= -\frac{\hbar}{2} e^{i3(\delta\psi_1 + \phi_1)} [\Omega_1 + \Omega_3 e^{i\theta}] e^{-i3\bar{\omega}_1 t} \\ &= U_{21}(t) e^{-i3\bar{\omega}_1 t}, \end{aligned} \quad (9)$$

where  $\Omega_1$  and  $\Omega_3$  are the Rabi frequencies associated with the  $\lambda_1$  and  $\lambda_3$  fields, respectively.

As discussed by Bonch-Bruевич and Khodovoi [16] the average excitation rate for an atom interacting with a stochastic field may be written in first order as [17]

$$\begin{aligned} \langle \Gamma(\theta_0, t) \rangle_1 &= \hbar^{-2} \int_0^t e^{-\gamma_2 |\tau|/2} \{ R(\tau) e^{i(\omega_{21} - 3\bar{\omega}_1)\tau} \\ &\quad + R^*(\tau) e^{-i(\omega_{21} - 3\bar{\omega}_1)\tau} \} d\tau, \end{aligned} \quad (10)$$

where  $\gamma_2$  is the decay rate of  $|2\rangle$  and  $R(\tau)$  is the autocorrelation function of the perturbation:

$$R(\tau) \equiv \langle U_{21}(t) U_{21}^*(t - \tau) \rangle. \quad (11)$$

Since we are only interested here in the case of  $3\bar{\omega}_1 = \omega_{21}$ , Eq. (10) becomes

$$\langle \Gamma(\theta_0, t) \rangle_1 = 2\hbar^{-2} \int_0^t \text{Re}[R(\tau)] e^{-\gamma_2 |\tau|/2} d\tau. \quad (12)$$

Then, substituting for  $U_{21}(t)$  in Eq. (11), we have

$$\begin{aligned} \langle \Gamma(\theta_0, t) \rangle_1 &= \frac{\Omega^2}{2} \int_0^t \text{Re} \{ \langle e^{i3\Lambda(\tau)} \rangle + e^{-i\theta_0} \langle e^{i3\Lambda(\tau)} e^{-i\alpha\delta\omega_1(0)} \rangle \\ &\quad + e^{i\theta_0} \langle e^{i3\Lambda(\tau)} e^{i\alpha\delta\omega_1(\tau)} \rangle \\ &\quad + \langle e^{i3\Lambda(\tau)} e^{i\alpha[\delta\omega_1(\tau) - \delta\omega_1(0)]} \rangle \} e^{-\gamma_2 |\tau|/2} d\tau, \end{aligned} \quad (13)$$

where we have set  $\Omega_1 = \Omega_3 = \Omega$ , and

$$\Phi_1(\tau) \equiv \delta\psi_1(\tau) - \delta\psi_1(0) = \int_0^\tau \delta\omega_1(t) dt, \quad (14a)$$

$$\delta\Phi_1(\tau) \equiv \delta\phi_1(\tau) - \delta\phi_1(0) = \left( \frac{n_1 L}{c} \right) [\delta\omega_1(\tau) - \delta\omega_1(0)], \quad (14b)$$

$$\Lambda(\tau) \equiv \Phi_1(\tau) + \delta\Phi_1(\tau). \quad (14c)$$

Note that the stochastic characteristics of  $\Lambda(\tau)$  define the third-harmonic-field spectrum at the exit of the dispersive medium. In particular, the first term in brackets on the right-hand side of Eq. (13) corresponds to the third-harmonic field's autocorrelation function. Thus, even in the absence of interfering pathways and phase control, the laser light's passage through the dispersive medium has an effect on the field-atom interaction by increasing the field's phase noise.

To proceed, we make the identifications

$$\langle e^{i3\Lambda(\tau)} e^{\pm i\alpha\delta\omega_1(t)} \rangle = \langle e^{i3\Lambda(\tau)} \rangle \langle e^{\pm i\alpha\delta\omega_1(t)} \rangle + C_{\pm}(\tau, t), \quad (15a)$$

$$\begin{aligned} \langle e^{i3\Lambda(\tau)} e^{i\alpha[\delta\omega_1(\tau) - \delta\omega_1(0)]} \rangle &= \langle e^{i3\Lambda(\tau)} \rangle \langle e^{i\alpha[\delta\omega_1(\tau) - \delta\omega_1(0)]} \rangle \\ &\quad + D(\tau, 0), \end{aligned} \quad (15b)$$

where

$$\begin{aligned} C_{\pm}(\tau, t) &\equiv \sum_{n,m=1}^{\infty} \frac{(i^{n+m})(\pm)^m}{n!m!} (3^n \alpha^m) [\langle \Lambda^n(\tau) \delta\omega_1^m(t) \rangle \\ &\quad - \langle \Lambda^n(\tau) \rangle \langle \delta\omega_1^m(t) \rangle] \end{aligned} \quad (16a)$$

and

$$D(\tau,0) \equiv \sum_{n,m=1}^{\infty} \frac{(i^{n+m})(3^n \alpha^m)}{n!m!} [\langle \Lambda^n(\tau) [\delta\omega_1(\tau) - \delta\omega_1(0)]^m \rangle - \langle \Lambda^n(\tau) \rangle \langle [\delta\omega_1(\tau) - \delta\omega_1(0)]^m \rangle]. \quad (16b)$$

Substituting Eqs. (15) into Eq. (13) then yields

$$\begin{aligned} \langle \Gamma(\theta_0, t) \rangle_1 &= \frac{\Omega^2}{2} \int_0^t \text{Re} \{ \langle e^{i3\Lambda(\tau)} [1 + e^{-i\theta_0} \langle e^{-i\alpha\delta\omega_1(0)} \rangle \\ &\quad + e^{i\theta_0} \langle e^{i\alpha\delta\omega_1(\tau)} \rangle + \langle e^{i\alpha[\delta\omega_1(\tau) - \delta\omega_1(0)]} \rangle] \\ &\quad + e^{-i\theta_0} C_-(\tau,0) + e^{i\theta_0} C_+(\tau, \tau) \\ &\quad + D(\tau,0) \rangle e^{-\gamma_2|\tau|/2} d\tau. \end{aligned} \quad (17)$$

The various correlation functions appearing in Eq. (17) are evaluated in the Appendix, and when these are substituted into Eq. (17) the expression simplifies to

$$\begin{aligned} \langle \Gamma(\theta_0, t) \rangle_1 &= \frac{\Omega^2}{2} \int_0^t \left\{ 2\mathcal{L}_3(\tau) \left[ \frac{1}{2} \{ 1 + \exp[-\alpha^2\gamma\beta(1 - e^{-\beta|\tau|})] \} + e^{-\alpha^2\gamma\beta} \cos[\theta_0] + e^{-i\theta_0} C_-(\tau,0) \right. \right. \\ &\quad \left. \left. + e^{i\theta_0} C_+(\tau, \tau) + D(\tau,0) \right\} e^{-\gamma_2|\tau|/2} d\tau, \end{aligned} \quad (18)$$

where  $\mathcal{L}_3(\tau)$  is the autocorrelation function of the third harmonic field at the exit of the dispersive medium. (The spectral characteristics of this field are discussed in the Appendix.)

To the extent that the correlation functions of Eqs. (15a) and (15b) are dominated by the first term on their respective right-hand sides, the field's frequency fluctuations (i.e., the  $\Lambda$  terms) are decorrelated from the fluctuations in the phase difference between the two fields [i.e., the  $\alpha\delta\omega_1(t)$  terms]. In this ‘‘decorrelation approximation,’’  $\langle \Gamma \rangle_1$  is very similar to  $\langle \Gamma \rangle_0$  except for the factor  $\{1 + \exp[-\alpha^2\gamma\beta(1 - e^{-\beta|\tau|})]\}$ . If, however, the atomic system's ‘‘memory’’ of the relative phase difference is short (i.e.,  $\gamma_2 \gg \beta$ ), then this factor can be evaluated at  $\tau = 0$  and removed from the integrand. In that case the zeroth-order approximation is essentially recovered.

The  $C_{\pm}$  and  $D$  terms in Eqs. (15a) and (15b) are corrections to the decorrelation approximation, and as seen via Eqs. (16) these will in general depend on very high order correlation functions associated with the field's frequency fluctuations. Note, however, that for a given value of  $m$  the summation coefficients are  $3^n/n!$ , and these are all of the same magnitude up to  $n \approx 7$ . Thus, though one might reasonably restrict  $C_{\pm}$  and  $D$  to  $m=1$  since  $\alpha$  is small, it would still be necessary to evaluate very high order correlation coefficients like  $\langle \Lambda^7(\tau)\delta\omega_1(t) \rangle$ . Thus, as a practical matter first-order perturbation theory is not particularly attractive for studying the effects of phase fluctuations on control. Nevertheless, the first-order perturbation theory results can be used to gain a *qualitative* understanding of field phase fluctuations and control.

In this vein, Fig. 2(a) shows a perturbation theory computation of the contrast  $\zeta$  as a function of field linewidth, where

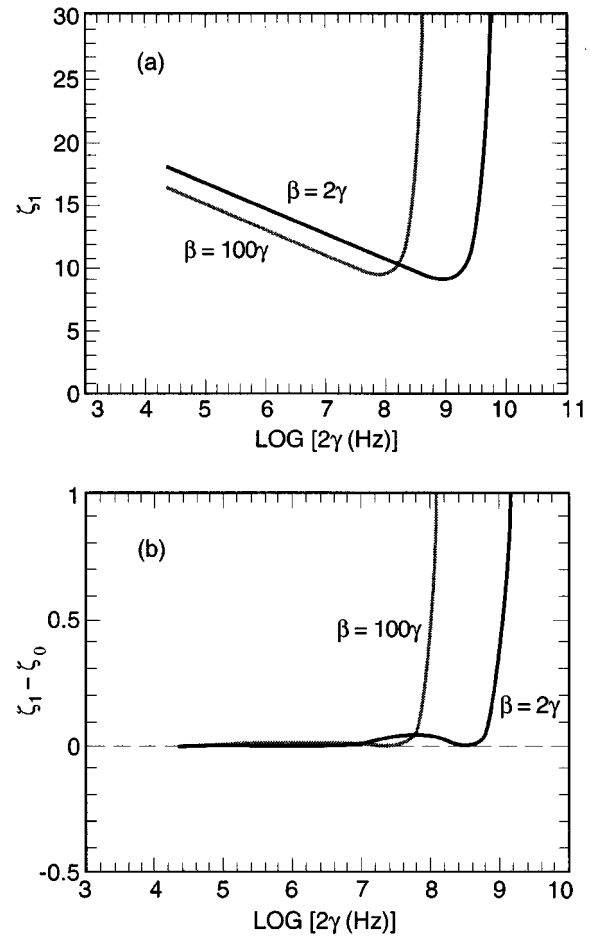


FIG. 2. Results from a first-order perturbation theory calculation, where  $n=m=1$  in Eqs. (16a) and (16b). (a)  $\zeta_1$  vs field linewidth,  $\log_{10}(2\gamma)$ , where  $\zeta_1$  is the contrast predicted by first-order perturbation theory. (b)  $\zeta_1 - \zeta_0$  vs field linewidth, where  $\zeta_0$  is the contrast predicted by the zeroth-order approximation.

the summations in Eqs. (16) were restricted to  $n=m=1$ . In the calculations we assumed a pulsed field with a pulsewidth of 1 nsec, and two calculations were performed corresponding to  $\beta=2\gamma$  and  $\beta=100\gamma$ . Note that  $\zeta \sim -\log_{10}[\gamma]$  for narrow linewidth fields, and that the contrast for  $\beta=2\gamma$  is larger than the contrast for  $\beta=100\gamma$ . Each of these observations is consistent with the zeroth-order approximation embodied by Eq. (8). At large values of  $\gamma$  the contrast diverges, indicating the importance of high order  $\langle \Lambda^n(\tau)\delta\omega_1(t) \rangle$  terms to the determination of contrast. This is shown more clearly in Fig. 2(b), where the difference in contrast between first-order perturbation theory and the zeroth-order approximation (i.e.,  $\zeta_1 - \zeta_0$ ) is plotted as a function of field linewidth. For the case of  $\beta=100\gamma$  agreement breaks down at about  $3 \times 10^7$  Hz while for  $\beta=2\gamma$  the agreement breaks down at about  $3 \times 10^8$  Hz.

#### IV. NUMERICAL SIMULATION

Given the limitations of first-order perturbation theory in calculating the effects of laser phase noise on control, in this section we will use the density-matrix equations describing phase control to investigate the problem. Employing the perturbation  $V^{(1,3)}$  defined in the preceding section, it is possible

to derive the following density matrix equations for phase control:

$$\left[ \frac{d}{dt} + i\Delta + \frac{1}{2} [\gamma_2 + \gamma_{\text{ion}}(t)] \right] \sigma_{12}(t) = \frac{i}{2} e^{-i3\delta\phi_1(t)} [\sigma_{22}(t) - \sigma_{11}(t)] [\Omega_1 + \Omega_3 e^{-i\theta(t)}], \quad (19a)$$

$$\begin{aligned} \frac{d}{dt} \sigma_{11}(t) = & \gamma_2 \sigma_{22}(t) + \cos(3\delta\phi_1(t)) \{ \text{Im}[\sigma_{12}(t)] \\ & \times [\Omega_1 + \Omega_3 \cos(\theta)] + \text{Re}[\sigma_{12}(t)] \Omega_3 \sin(\theta) \} \\ & + \sin(3\delta\phi_1(t)) \{ \text{Re}[\sigma_{12}(t)] [\Omega_1 + \Omega_3 \cos(\theta)] \\ & - \text{Im}[\sigma_{12}(t)] \Omega_3 \sin(\theta) \}, \end{aligned} \quad (19b)$$

$$\begin{aligned} \left[ \frac{d}{dt} + \gamma_2 + \gamma_{\text{ion}}(t) \right] \sigma_{22}(t) = & -\cos(3\delta\phi_1(t)) \{ \text{Im}[\sigma_{12}(t)] \\ & \times [\Omega_1 + \Omega_3 \cos(\theta)] \\ & + \text{Re}[\sigma_{12}(t)] \Omega_3 \sin(\theta) \} \\ & - \sin(3\delta\phi_1(t)) \{ \text{Re}[\sigma_{12}(t)] \\ & \times [\Omega_1 + \Omega_3 \cos(\theta)] \\ & - \text{Im}[\sigma_{12}(t)] \Omega_3 \sin(\theta) \}. \end{aligned} \quad (19c)$$

Here,

$$\Delta \equiv (3\bar{\omega}_1 - \omega_{21}) + 3\delta\omega_1(t) - \kappa I_1(t), \quad (19d)$$

with  $3\bar{\omega}_1 - \omega_{21}$  the field detuning from the unperturbed three-photon resonance,  $\kappa I_1(t)$  the ac Stark shift due to the three-photon excitation, and  $I_1(t)$  the pulsed intensity of the  $\lambda_1$  field. (All calculations to be discussed below were performed with  $3\bar{\omega}_1 = \omega_{21}$ .) The  $\sigma_{ij}(t)$  are the usual slowly varying parts of the density matrix, and  $\gamma_{\text{ion}}(t)$  is the ionization rate of state  $|2\rangle$  given by  $\hat{\sigma}_2 I_1^2(t)$  with  $\hat{\sigma}_2$  the generalized two-photon ionization cross section of  $|2\rangle$ . Further,  $\Omega_i$  is the Rabi frequency corresponding to the  $\lambda_i$  field, and again we set  $\Omega_1$  equal to  $\Omega_3$  so as to maximize the contrast between constructive and destructive interference.

Following our previously outlined Monte Carlo methodology [18], we generate a realization of the field's frequency fluctuations, and then numerically integrate the density matrix equations for a 1-ns Gaussian pulse using a Runge-Kutta-Fehlberg technique [19]. Our signal,  $S(\theta_0)$ , is the total ionization produced by the field during the pulse, which is simply calculated as

$$S(\theta_0) = \int_0^{2\tau} \gamma_{\text{ion}}(t) \sigma_{22}(t, \theta_0) dt, \quad (20)$$

where  $\tau$  is the 1-ns field pulsewidth (field intensity FWHM). (In the numerical simulation the Gaussian pulse only lasts for  $0 \leq t \leq 2\tau$ .)

### Weak-field results

Figure 3 shows the results of our density-matrix calculation for  $I_1(\text{peak}) = 10^8 \text{ W/cm}^2$ ; specifically, the constructive

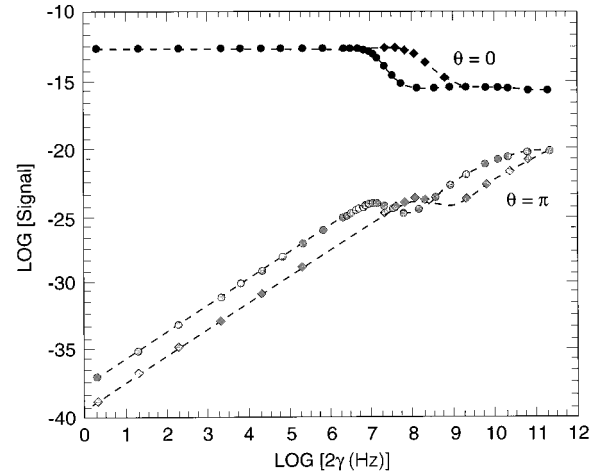


FIG. 3. Numerical simulation results showing the photoionization signal produced by a 1-ns pulse as a function of field linewidth,  $2\gamma$ . Circles correspond to  $\beta=100\gamma$ , while diamonds correspond to  $\beta=2\gamma$ ; logarithms are base 10.

and destructive signals vs field linewidth. From the data in Table I, it is clear that at this intensity the three-photon Rabi frequency is less than the decay rate of the  $6s[3/2]_1$  state,  $\gamma_2$ . Additionally, the peak ac Stark shift of the transition is not quite equal to the transform limited bandwidth of the pulsed field. Consequently, for the sake of clarity in comparing the numerical results to first-order perturbation theory, we chose to set the ac Stark shift coefficient to zero in the weak field calculations. Circles correspond to the case  $\beta=100\gamma$ , while the diamonds correspond to the case  $\beta=2\gamma$ . For narrow linewidth fields the constructive interference signal is essentially constant, while the destructive interference signal is proportional to  $\gamma^2$ . Moreover, consistent with first-order perturbation theory this behavior changes at linewidths of roughly  $3 \times 10^7 \text{ Hz}$  and  $3 \times 10^8 \text{ Hz}$  for  $\beta=100\gamma$  and  $\beta=2\gamma$ , respectively.

Figure 4(a) shows our density-matrix results of the contrast vs field linewidth, where  $\zeta \equiv \log_{10}[S(0)/S(\pi)]$ . Here, black circles correspond to  $\beta=100\gamma$  while gray circles correspond to  $\beta=2\gamma$ , and the dashed line corresponds to the zeroth-order approximation. Perhaps the most noteworthy conclusion to be drawn from the results is that even for fields with a linewidth of  $3 \text{ cm}^{-1}$  (i.e., 90 GHz), the contrast is very high (i.e.,  $\zeta \sim 5$ ). Thus, excellent phase control should be possible with PDF's of large linewidth. Note also that the density matrix results are in very good agreement with the zeroth-order approximation up to these large linewidth fields. This is shown more clearly in Fig. 4(b) where  $\zeta - \zeta_0$  is plotted as a function of field linewidth. Based on the results shown in Fig. 2, the agreement between  $\zeta$  and  $\zeta_0$  is somewhat unexpected, and suggests that successive summation terms associated with the  $C_{\pm}$  and  $D$  corrections to the decorrelation approximation have a mitigating influence on one another.

A breakdown in the agreement between  $\zeta$  and  $\zeta_0$  is noticeable in Fig. 4(b) but only for field linewidths larger than the transform limited width of the pulse. This is a consequence of the conflicting influence of field frequency fluctuations on the destructive interference signal. Crudely, one can write the destructive interference signal as

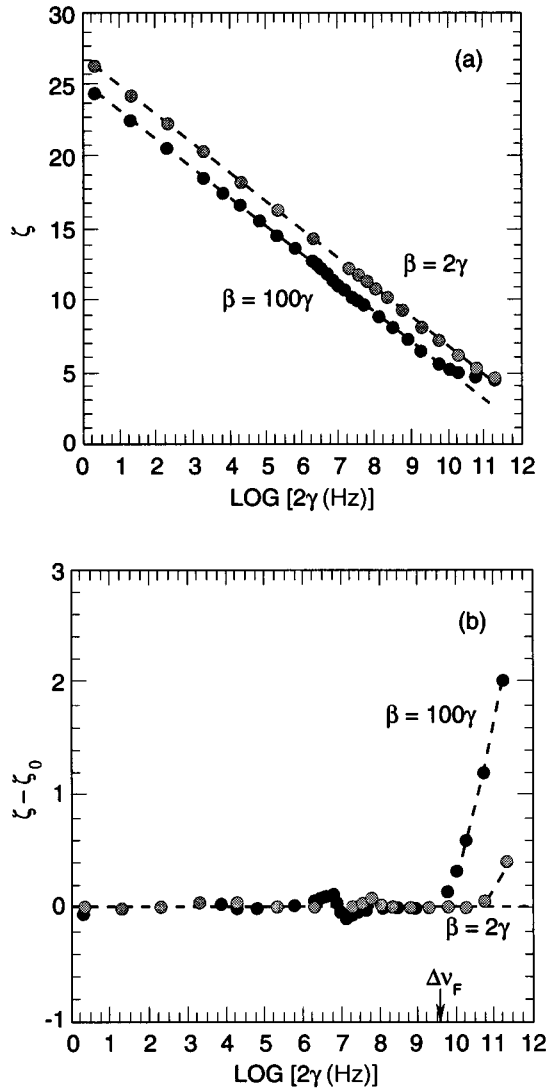


FIG. 4. Numerical simulation results of contrast  $\zeta$  for a weak field [i.e.,  $I_1(\text{peak})=10^8 \text{ W/cm}^2$ ]. (a)  $\zeta$  vs field linewidth,  $2\gamma$ . Black circles correspond to  $\beta=100\gamma$ , while gray circles correspond to  $\beta=2\gamma$ . The dashed line is the zeroth-order approximation,  $\zeta_0$ . (b)  $\zeta - \zeta_0$  vs field linewidth. Again, black circles correspond to  $\beta=100\gamma$ , while gray circles correspond to  $\beta=2\gamma$ ;  $\Delta\nu_F$  corresponds to the transform limited linewidth (FWHM) of the 1-ns pulse. Logarithms are base 10.

$$\Gamma(\pi) = \frac{1}{2} \frac{\Omega^2(1 + \cos[\pi + \delta\theta])^2}{9\gamma + \Delta\omega_F/2} = \frac{1}{4} \frac{\Omega^2[\alpha\delta\omega_1]^2}{9\gamma + \Delta\omega_F/2}, \quad (21a)$$

$$\langle \Gamma(\pi) \rangle = \frac{1}{4} \frac{\Omega^2\alpha^2\gamma\beta}{9\gamma + \Delta\omega_F/2}, \quad (21b)$$

where  $\Delta\omega_F$  is the transform limited bandwidth of the pulsed field (FWHM), and the factor of 9 in the denominator multiplying  $\gamma$  comes from the three-photon nature of the transition [13]. For  $\gamma \ll \Delta\omega_F$  the field's frequency fluctuations increase the average rate of destructive interference excitation, and contrast follows the zeroth-order approximation. However, when  $\gamma \gg \Delta\omega_F$ , then field frequency fluctuations play an additional role, since the field's instantaneous detuning

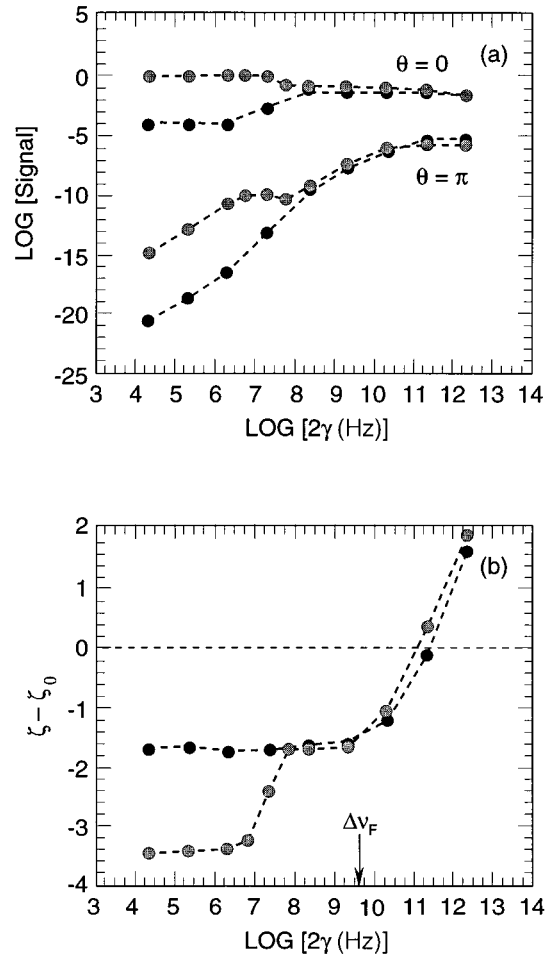


FIG. 5. Numerical simulation results of contrast  $\zeta$  for a strong field [i.e.,  $I_1(\text{peak})=10^{11} \text{ W/cm}^2$ ], and where  $\beta=100\gamma$ . (a) Signal vs field linewidth,  $2\gamma$ . Black circles correspond to an ac Stark shift coefficient,  $\kappa$ , of  $36 \text{ cm}^2/(\text{W sec})$ , while gray circles correspond to  $\kappa=0$ . The dashed line is simply meant as an aid to guide the eye. (b)  $\zeta - \zeta_0$  vs field linewidth. Again, black circles correspond to  $\kappa=36 \text{ cm}^2/(\text{W sec})$ , while gray circles correspond to  $\kappa=0$ ;  $\Delta\nu_F$  corresponds to the transform limited linewidth (FWHM) of the 1-ns pulse. Logarithms are base 10.

from resonance decreases the destructive interference excitation rate. The net result is a smaller average destructive interference signal than that predicted by the zeroth-order approximation, and hence a relatively larger contrast.

### Strong-field results

For comparative purposes and completeness, Fig. 5 shows our results of the photoionization signal and  $\zeta - \zeta_0$  as a function of field linewidth for a strong field [i.e.,  $I_1(\text{peak})=10^{11} \text{ W/cm}^2$ ]. The signal again was computed via Eq. (20). Two cases are shown: black circles correspond to an ac Stark shift coefficient, of  $36 \text{ cm}^2/(\text{W sec})$ , while gray circles correspond to  $\kappa=0$ . In narrow linewidth fields with  $\kappa=0$  the photoionization signal is saturated, and as one might expect the computed contrast is less than that predicted by the zeroth-order approximation. With  $\kappa=36 \text{ cm}^2/(\text{W sec})$ , the dynamic detuning of the levels does not allow for saturation of the photoionization signal, and the contrast is somewhat increased in narrow linewidth fields though still less than that predicted

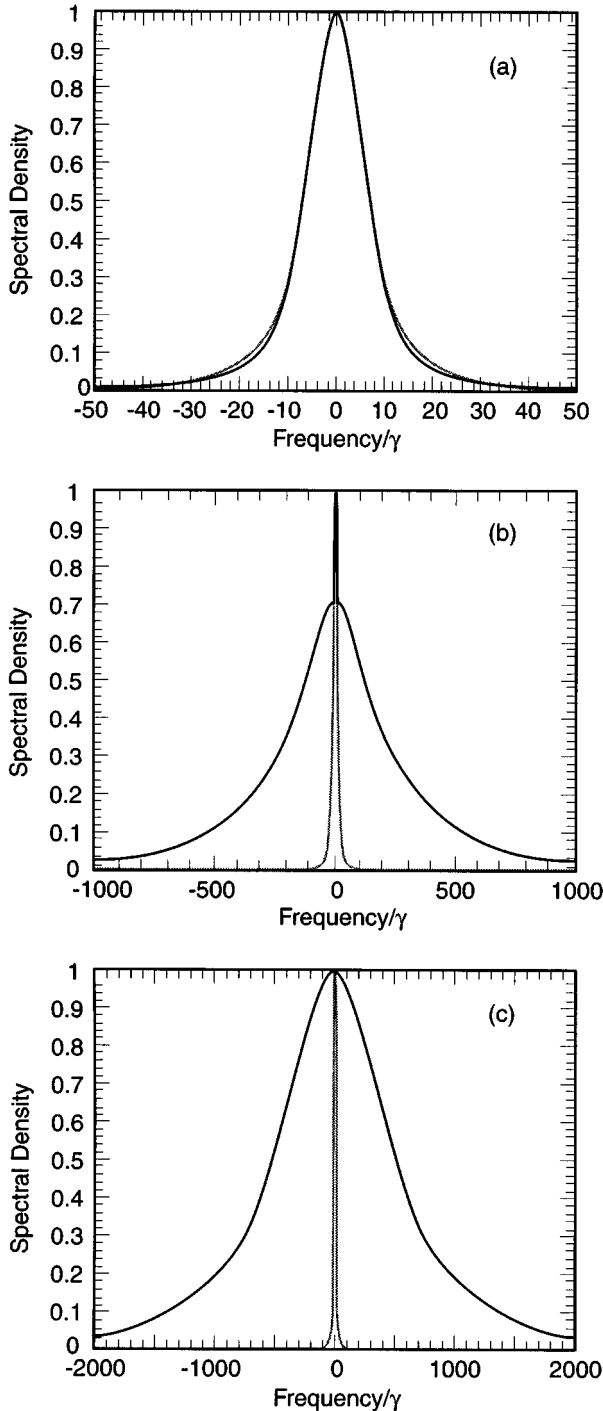


FIG. 6. Spectral density of the third harmonic field prior to passage through the dispersive medium (gray curve) and after passage through the dispersive medium (black curve). For these illustrative results  $\beta=30\gamma$  and  $L=50$  cm. (a)  $\gamma=1.0\times 10^7$  Hz; (b)  $\gamma=1.5\times 10^7$  Hz; (c)  $\gamma=3.0\times 10^7$  Hz.

by the zeroth-order approximation. Again, as the linewidth becomes larger than the pulse's transform limited bandwidth,  $\Delta\omega_F$ , the contrast becomes larger than that predicted by the zeroth-order approximation.

## V. CONCLUSIONS

We have considered 3+1 phase control with a PDF from three perspectives: (i) a physically intuitive zeroth-order ap-

proximation, (ii) first-order perturbation theory, and (iii) numerical simulation. Our results have shown that in narrow linewidth PDF's all three approaches yield the same value for the contrast, indicating the utility of the zeroth-order approximation in this regime. In broad linewidth fields the zeroth-order approximation breaks down. However, since the zeroth-order approximation tends to *underestimate* the degree of control (i.e., contrast  $\zeta$ ) in the cases studied here, it may still be of value in the broad linewidth PDF regime. The breakdown of the zeroth-order approximation is a consequence of very high order correlation functions associated with the fundamental field's fluctuating frequency, as shown by our first-order perturbation theory analysis of the problem. Moreover, these high-order correlation functions limit the utility of first-order perturbation theory, and highlight the necessity of numerical simulation for an accurate treatment of phase control with a stochastic field.

Perhaps the most interesting result from the present studies concerns the magnitude of contrast obtained with a PDF. Even for PDF's with linewidths on the order of  $\text{cm}^{-1}$ , our results show four to five orders of magnitude difference between constructive and destructive interference signals. This degree of contrast has yet to be realized in any phase-control experiment, and clearly indicates that the experimental limitations to phase control do not come from the laser's phase fluctuations. As suggested by a number of authors, the laser beam's spatial profile may have an important influence on the observed degree of phase control. Additionally, as the experiments done to date have employed multimode lasers, field amplitude fluctuations could play an important role in limiting phase control. We intend to address this latter issue in future numerical simulations of the phase-control problem.

## ACKNOWLEDGMENT

This work was supported under the Aerospace Sponsored Research Program.

## APPENDIX

### Evaluation of $\langle \exp[-in\Lambda(\tau)] \rangle$

Following a procedure discussed by Jacobs [20], we define  $P_\Lambda(\tau)$  as the probability density of  $\Lambda$  at time delay  $\tau$ . Thus,

$$\langle e^{-in\Lambda(\tau)} \rangle = \int_{-\infty}^{\infty} P_\Lambda(\tau) e^{-in\Lambda} d\Lambda. \quad (\text{A1})$$

Then, taking  $\Lambda$  to be Gaussian distributed

$$\langle e^{-in\Lambda(\tau)} \rangle = \frac{1}{\sigma(\tau)\sqrt{2\pi}} \int_{-\infty}^{\infty} e^{-\Lambda^2/2\sigma^2(\tau)} e^{-in\Lambda} d\Lambda, \quad (\text{A2})$$

where  $\sigma^2(\tau)$  is the variance of  $\Lambda$  at delay  $\tau$ . Completing the square of the integrand and integrating finally yields

$$\langle e^{-in\Lambda(\tau)} \rangle = e^{-n^2\sigma^2(\tau)/2}. \quad (\text{A3})$$

To proceed, it is necessary to determine the variance of  $\Lambda$ , and with the aid of Eqs. (6b) and (14) we obtain

$$\sigma^2(\tau) = \langle \Phi_1^2(\tau) \rangle + \langle \delta\Phi_1^2(\tau) \rangle + 2\langle \Phi_1(\tau) \delta\Phi_1(\tau) \rangle, \quad (\text{A4a})$$

$$\langle \Phi_1^2(\tau) \rangle = \frac{2\gamma}{\beta} [\beta|\tau| - 1 + e^{-\beta|\tau|}], \quad (\text{A4b})$$

$$\langle \delta\Phi_1^2(\tau) \rangle = 2 \left( \frac{n_1 L}{c} \right)^2 \gamma\beta [1 - e^{-\beta|\tau|}], \quad (\text{A4c})$$

and

$$\langle \Phi_1(\tau) \delta\Phi_1(\tau) \rangle = 0. \quad (\text{A4d})$$

Note that  $\langle e^{-i3\Lambda(\tau)} \rangle$  is the correlation function of the third harmonic field,  $\mathcal{L}_3(\tau)$ , after it has exited the dispersive medium. Consequently, the Fourier transform of  $\mathcal{L}_3(\tau)$  is the third harmonic field spectrum,  $\mathcal{L}_3(\omega)$ , at the exit of the dispersive medium. Examples of this field spectrum are shown in Fig. 6 for the case of  $\beta=30\gamma$ , and  $L=50$  cm, where the black curve corresponds to the third harmonic field spectrum at the exit of the dispersive medium and the gray curve corresponds to the third harmonic field spectrum at the entrance to the dispersive medium. Note that for  $\gamma < 10^7$  Hz the dispersive medium has little effect on the third harmonic field line shape, while for  $\gamma > 3 \times 10^7$  Hz the line shape is primarily influenced by the field's passage through the dispersive medium. Thus, not only does the dispersive medium give rise to relative phase fluctuations between the fundamental and third harmonic fields, it also has a significant effect on both the fundamental and third harmonic field line shapes.

#### Evaluation of $\langle \exp[\pm i\alpha\delta\omega_1(t)] \rangle$

By definition,

$$\langle \exp[\pm i\alpha\delta\omega_1(t)] \rangle = \int_{-\infty}^{\infty} P(\delta\omega_1; t) \exp[\pm i\alpha\delta\omega_1] d[\delta\omega_1], \quad (\text{A5})$$

where  $P(\delta\omega_1; t)$  is the probability density of the  $\delta\omega_1$  at time  $t$ . Since  $\delta\omega_1$  represents a stationary random process,  $P(\delta\omega_1; t)$  is independent of  $t$  and given by Eq. (6a). Thus,

$$\langle \exp[\pm i\alpha\delta\omega_1(t)] \rangle = \frac{1}{\sigma} \left( \frac{2}{\pi} \right)^{1/2} \int_0^{\infty} e^{-x^2/2\sigma^2} \cos[\alpha x] dx, \quad (\text{A6})$$

where  $x$  is a dummy variable replacing  $\delta\omega_1$ , and  $\sigma^2$  is the variance of  $\delta\omega_1$  given by Eq. (6b) as  $\gamma\beta$ . Evaluating the integral then yields

$$\langle \exp[\pm i\alpha\delta\omega_1(t)] \rangle = e^{-\alpha^2\gamma\beta/2}. \quad (\text{A7})$$

#### Evaluation of $\langle \exp[i\alpha(\delta\omega_1(\tau) - \delta\omega_1(0))] \rangle$

For ease of notation we define  $x$  and  $y$  as  $\delta\omega_1(\tau)$  and  $\delta\omega_1(0)$ , each with variance  $\gamma\beta$ , and note that the correlation between  $x$  and  $y$ , defined as  $r$ , is just  $\gamma\beta e^{-\beta|\tau|}$ . Then, taking  $x$  and  $y$  to be jointly normal, we can define two new random variables,  $w$  and  $z$ , which will also be jointly normal:  $w \equiv x + y$  and  $z \equiv x - y$ .

From Papoulis[21] we have for the joint probability density of  $w$  and  $z$ ,  $P_{wz}$ :

$$P_{wz} = \frac{1}{4\pi\gamma\beta\sqrt{1-r^2}} \exp\left[-\frac{z^2}{4\gamma\beta(1-r)}\right] \times \exp\left[-\frac{w^2}{4\gamma\beta(1+r)}\right], \quad (\text{A8})$$

and after integrating over  $w$  this gives the probability density of  $z$ :

$$P_z = \frac{1}{2\sqrt{\gamma\beta\pi(1-r)}} \exp\left[-\frac{z^2}{4\gamma\beta(1-r)}\right]. \quad (\text{A9})$$

With the aid of Eq. (A9) the correlation function is easily evaluated:

$$\langle \exp\{i\alpha[\delta\omega_1(\tau) - \delta\omega_1(0)]\} \rangle = \int_{-\infty}^{\infty} e^{iaz} P_z dz, \quad (\text{A10})$$

and after substituting from Eq. (A9) and integrating this yields

$$\langle \exp\{i\alpha[\delta\omega_1(\tau) - \delta\omega_1(0)]\} \rangle = \exp[-\alpha^2\gamma\beta(1 - e^{-\beta|\tau|})]. \quad (\text{A11})$$

- 
- [1] M. Shapiro, J. W. Hepburn, and P. Brumer, Chem. Phys. Lett. **149**, 451 (1988); P. Brumer and M. Shapiro, Acc. Chem. Res. **22**, 407 (1989); C. K. Chan, P. Brumer, and M. Shapiro, J. Chem. Phys. **94**, 2688 (1991).
- [2] We note that the 3+1 mechanism had been proposed previously as an explanation for the suppression of three-photon excitation in dense atomic vapors. See, for example, D. J. Jackson and J. J. Wynne, Phys. Rev. Lett. **49**, 543 (1982).
- [3] C. Chen, Y. Yan, and D. S. Elliot, Phys. Rev. Lett. **64**, 507 (1990); C. Chen and D. S. Elliot, *ibid.* **65**, 1737 (1990).
- [4] S. M. Park, S-P. Lu, and R. J. Gordon, J. Chem. Phys. **94**, 8622 (1991); S-P. Lu, S. M. Park, Y. Xie, and R. J. Gordon, *ibid.* **96**, 6613 (1992).
- [5] A. D. Bandrauk and J-M. Gauthier, Chem. Phys. Lett. **200**, 399 (1992).
- [6] V. D. Kleiman, L. Zhu, X. Li, and R. J. Gordon, J. Chem. Phys. **102**, 5863 (1995).
- [7] R. J. Gordon, S-P. Lu, S. M. Park, K. Trentelman, Y. Xie, and L. Zhu, J. Chem. Phys. **98**, 9481 (1993).
- [8] T. Nakajima, P. Lambropoulos, S. Cavalieri, and M. Matera, Phys. Rev. A **46**, 7315 (1992).
- [9] T. Nakajima and P. Lambropoulos, Phys. Rev. Lett. **70**, 1081 (1993).
- [10] P. J. Leonard, At. Data Nucl. Data Tables **14**, 21 (1974).
- [11] G. I. Chashchina and E. Ya. Shreider, Opt. Spektrosk. **27**, 161 (1969).

- [12] For a discussion of MQDT in this context, see A. L'Huillier, X. Tang, and P. Lambropoulos, *Phys. Rev. A* **39**, 1112 (1989).
- [13] P. Zoller and P. Lambropoulos, *J. Phys. B* **12**, L547 (1979).
- [14] A. T. Georges and P. Lambropoulos, in *Advances in Electronics and Electron Physics* (Academic, New York, 1980), Vol. 54, pp. 191–240; L. Allen and C. R. Stroud, Jr., *Phys. Rep.* **91**, 1 (1982).
- [15] P. Lambropoulos and X. Tang, in *Atoms in Intense Laser Fields*, edited by M. Gavrila (Academic, Boston, 1992), pp. 335–372.
- [16] A. M. Bonch-Bruевич and V. A. Khodovoi, *Usp. Fiz. Nauk* **85**, 3 (1965) [*Sov. Phys. Usp.* **8**, 1 (1965)].
- [17] Note that since we are concerned with weak fields, we have ignored the ac Stark shift of the two coupled levels.
- [18] J. C. Camparo and P. Lambropoulos, *Phys. Rev. A* **47**, 480 (1993).
- [19] W. Cheney and D. Kincaid, in *Numerical Mathematics and Computing* (Brooks Cole, Monterey, CA, 1985); W. H. Press and S. A. Teukolsky, *Comp. Phys.* **6**, 188 (1992).
- [20] S. F. Jacobs, *Am. J. Phys.* **47**, 597 (1979).
- [21] A. Papoulis, *Probability, Random Variables, and Stochastic Processes* (McGraw-Hill, New York, 1965), Chap. 7.